Drosophila, which lacks canonical transcription-coupled repair proteins, performs transcription-coupled repair

Received for publication, October 10, 2019, and in revised form, October 16, 2019 Published, Papers in Press, October 17, 2019, DOI 10.1074/jbc.AC119.011448

Nazli Deger[‡1,2], Yanyan Yang[§1], Laura A. Lindsey-Boltz[§], Aziz Sancar[§3], and Christopher P. Selby[§4]

From the Departments of [‡]Biology and [§]Biochemistry and Biophysics, University of North Carolina at Chapel Hill, North Carolina 27599

Edited by Patrick Sung

Previous work with the classic T4 endonuclease V digestion of DNA from irradiated *Drosophila* cells followed by Southern hybridization led to the conclusion that *Drosophila* lacks transcription-coupled repair (TCR). This conclusion was reinforced by the *Drosophila* Genome Project, which revealed that *Drosophila* lacks Cockayne syndrome WD repeat protein (CSA), CSB, or UV-stimulated scaffold protein A (UVSSA) homologs, whose orthologs are present in eukaryotes ranging from *Arabidopsis* to humans that carry out TCR. A recently developed *in vivo* excision assay and the excision repair-sequencing (XR-Seq) method have enabled genome-wide analysis of nucleotide excision repair in various organisms at single-nucleotide resolution and in a strand-specific manner. Using these methods, we have discovered that *Drosophila* S2 cells carry out robust TCR comparable with that observed in mammalian cells. Our findings provide critical new insights into the mechanisms of TCR among various different species.

Nucleotide excision repair (excision repair) is the main mechanism used by many organisms to remove cyclobutane pyrimidine dimers (CPDs)[5] that are induced in DNA by UV light (1, 2). The mechanism of excision repair has been investigated in considerable detail in several model organisms including *Escherichia coli*, *Saccharomyces cerevisiae*, mice, humans, and more recently *Arabidopsis thaliana* (3, 4). In contrast, although *Drosophila melanogaster* is an extensively used model organism that has contributed significantly to the development of modern views on ionizing radiation and chemical mutagenesis and to the development of double-strand break repair and recombination models (5), there is rather limited information on nucleotide excision repair in this organism.

Work on excision repair in *Drosophila* is of special interest because, of all of the model organisms studied, ranging from *E. coli* to humans, it is the only one that has been reported to lack transcription-coupled repair (TCR) (6–10). This conclusion was further supported by genomic analyses that revealed that the CSA and CSB proteins, which are necessary for TCR (11) and are present in organisms ranging from yeast (Rad28 and Rad26, respectively) to humans, are missing in *Drosophila* and other insects in the order Diptera (5, 12, 13). Considering the importance of TCR in mutation avoidance (14), the apparent absence of TCR in *Drosophila* is rather surprising. Therefore, we decided to investigate this phenomenon with new biochemical tools that have become available since the previous experimental studies on the subject nearly 3 decades ago.

In transcription-coupled repair, damage in the template (transcribed strand (TS)), but not the nontranscribed strand (NTS), causes arrest of RNA polymerase (RNAP). The arrested RNAP is recognized by Mfd in *E. coli* (15, 16) and by CSB in eukaryotes (17). The bacterial TCR process is well-characterized and involves concerted removal of RNAP by the Mfd translocase and Mfd-mediated delivery of repair proteins, resulting in repair at an accelerated rate compared with repair of the NTS (15). In contrast, TCR is not well-understood in higher organisms. The mechanism is unlike that in *E. coli*, because the CSB translocase does not remove the stalled RNAP (18). Nevertheless, CSB, along with CSA, a WD repeat–containing protein with ubiquitin ligase activity (19), somehow enables the eukaryotic basal repair proteins (which are not homologous to proteins in *E. coli*) to produce a commonly 3–10-fold accelerated rate of TS repair, which varies depending upon the level of transcription (14, 16, 20).

In the classic TCR assay (14), UV-irradiated cells are incubated for various times to allow repair and then harvested. Genomic DNA is isolated and digested with appropriate restriction enzymes, and then duplicate aliquots from each time point are incubated with or without T4 endonuclease V, which incises sites of CPDs. Following separation of the DNA on a denaturing agarose gel, the gel is probed with gene-specific and strand-specific probes. The level of damage at each time point is calculated from the decrease in full-length fragment caused by T4 endonuclease. The loss of damage with time represents repair. Although this method has served to characterize essential properties of strand-specific repair, by its very nature, it is

This work was supported by National Institutes of Health Grants GM118102 and ES027255 (to A. S.). The authors declare that they have no conflicts of interest with the contents of this article. The content is solely the responsibility of the authors and does not necessarily represent the official views of the National Institutes of Health.

The raw data and alignment data have been deposited in the Gene Expression Omnibus under accession numbers GSE76391, GSE67941, and GSE138846.

[1] Both authors contributed equally to this work.

[2] Supported by the Turkish Fulbright Commission.

[3] To whom correspondence may be addressed. E-mail: aziz_sancar@med.unc.edu.

[4] To whom correspondence may be addressed. E-mail: cselby@med.unc.edu.

[5] The abbreviations used are: CPD, cyclobutane pyrimidine dimer; TCR, transcription-coupled repair; XR-Seq, excision repair sequencing; TS, transcribed strand or template strand; NTS, nontranscribed strand or coding strand; NGS, next-generation sequencing; TSS, transcription start site; TES, transcription end site; CSA and CSB, Cockayne Syndrome group A and B, respectively; RPKM, reads per kbp per million total reads; RNAP, RNA polymerase; nt, nucleotide(s); UVSSA, UV-stimulated scaffold protein A.

© 2019 Deger et al. Published under exclusive license by The American Society for Biochemistry and Molecular Biology, Inc.

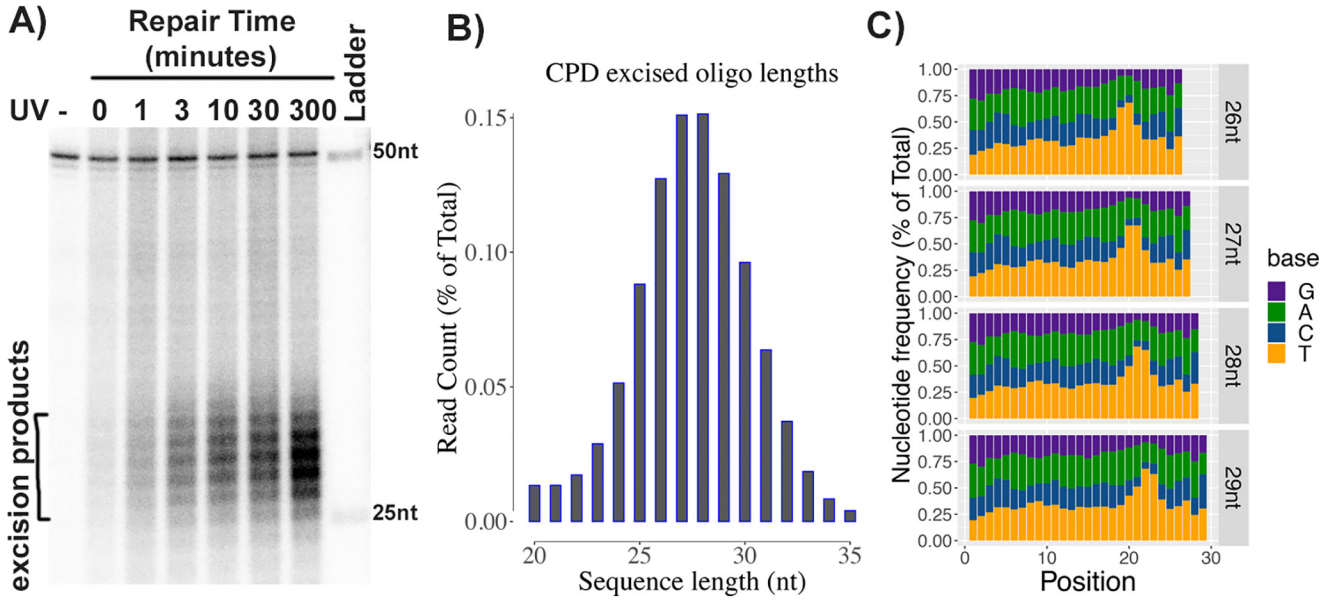

Figure 1. *In vivo* excision assay and XR-Seq analysis in *Drosophila*. *A*, *in vivo* excision assay. S2 cells were irradiated with 20 J/m^2 UV and incubated at 27 °C for 0–5 h. Then cells were lysed by the Hirt procedure, and low-molecular weight DNA in the supernatant was immunoprecipitated with anti-CPD antibodies. The oligonucleotides recovered were mixed with a 50-mer internal control oligonucleotide, 3′-end–labeled, and separated on a DNA-sequencing gel along with size markers. The excised oligomers are 24–32 nt in length, as is the case in human excision repair. *B*, size distribution of excised oligonucleotides as determined by XR-Seq analysis. A range of 24–32 and median of 27–28 nt was found. *C*, dual incision site determination by the distribution of thymine nucleotide in the reads. Frequency distribution of the 4 nucleotide bases in the 26-, 27-, 28-, and 29-nt-long reads as determined by XR-Seq is plotted. Potential T-T dinucleotides peak ~6–8 nucleotides from the 3′-end and 21–23 nucleotides from the 5′-terminus.

low-resolution and has the potential of missing TCR because it is an indirect method that is based on subtracting two large numbers from one another and because it is limited to analyzing one gene at a time. In contrast, the recently developed XR-Seq (excision repair-sequencing) assay directly captures and identifies the excised oligomers, and thus it directly and simultaneously measures repair throughout the genome (4, 20). Using XR-Seq, we find that *Drosophila* is proficient at TCR despite the previous reports and the absence of CSA and CSB in this organism.

Results

Excision by dual incision in Drosophila

Drosophila S2 cells were irradiated with 20 J m^{-2} of 254-nm UV light and incubated for various times at 27 °C. Then cells were lysed, and the low-molecular weight DNA was separated from genomic DNA by the Hirt procedure (4). After immunoprecipitation with anti-CPD antibodies, the samples were mixed with an internal control 50-mer DNA oligonucleotide, 3′-end–labeled, and separated on a sequencing gel. As seen in Fig. 1*A*, excision products in the range of 24–30 nt were detected with a median of 27–28 nt.

Irradiated S2 cells were also processed for XR-Seq, in which the excision products are isolated, repaired by CPD photolyase, sequenced by next-generation sequencing (NGS), and aligned to the genome to create a map of the entire genome showing sites of repair in both strands at single-nucleotide resolution. The lengths of excision products sequenced (reads) after 10 min of repair were recovered with the frequency distribution shown in Fig. 1*B*, which shows a peak at 27 and 28 nt, in agreement with Fig. 1*A* results. Reads for products 26, 27, 28, and 29 nt in length were individually analyzed for nucleotide distribution as shown in Fig. 1*C*. The results show enrichment of pyrimidines 7–9 nt from the 3′-end. Thymines are more common than cytosines, consistent with the prevalence of cyclobutane thymine dimer photoproducts produced by UV. Thus, the location of the dual incisions made by the excision nuclease with respect to the CPD in S2 cells is essentially the same as in humans (3, 20). This finding is not surprising, considering that *Drosophila* possesses the complete set of orthologs to the basal excision repair factors present in mammals (5). It is worth noting that in human cells, it has been shown that the same excision pattern is produced by the transcription-coupled and global repair pathways (20).

Processing of the excised oligomers

In humans (20, 21), yeast (22), and *Arabidopsis* (23, 24), the CPD-containing oligomers are rapidly processed by exonuclease(s) such that the primary excision product has a half-life of about 1 h. As repair progresses, two populations of excision products, one ranging from 24 to 32 nt and centering at 26–27 nt and a second in the range of 15–20 nt and centering at 17–18 nt, are observed. These products as produced in NHF1 cells are illustrated in Fig. 2*A*. The 15–20-nt degradation products can be seen even at the earliest time point of 30 min and become prominent at 2 h. Thereafter, both the primary and secondary excision products detectable by radiolabeling decline, presumably due to low recovery and labeling efficiency of smaller degraded CPD-containing oligonucleotides (not shown). A comparison of the fate of excised oligomers in human and *Drosophila* cells (Fig. 2*B*) reveals an interesting contrast; in S2 cells, no degradation products are detectable in the first 2 h and, in fact, up to at least 12 h (data not shown). This indicates that *Drosophila* either lacks a nuclease that is present in organisms

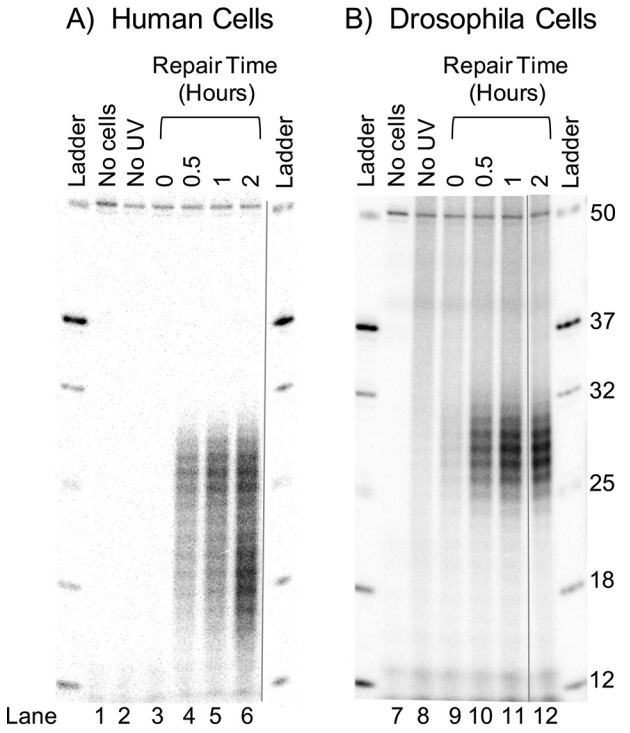

Figure 2. Nucleolytic processing of the excised oligonucleotides in human and *Drosophila* cells. Human NHF1 and *Drosophila* S2 cells were irradiated with 10 Jm^{-2} of 254-nm UV and incubated at 37 °C (human) or 27 °C (*Drosophila*) for the indicated times. Then the excised oligonucleotides were isolated, mixed with a 50-mer internal control, 3′-end labeled, and separated on DNA-sequencing gels. Shown are NHF1 (*A*) and S2 (*B*) cell excision products. Note that in NHF1 cells, the excised oligomers are degraded significantly by 2 h so that at this time point two classes of oligomers are seen, those centering at 26–27 nt (primary excision product) and those centering at 18–19 nt (degradation products). In contrast, in S2 cells, the size distribution of the excision products does not change with time.

ranging from yeast to *Arabidopsis* to humans and that generates a similar degradation pattern in all of these other species, or this degradation intermediate is not stabilized in *Drosophila* as it is in other organisms.

Transcription-coupled repair in Drosophila

Previous work using strand-specific Southern hybridization did not detect a difference in the rates of repair of TS and NTS in individual *Drosophila* genes (6–8), and it was concluded that *Drosophila* does not perform TCR. This notion was further strengthened by genome analyses, which revealed that *Drosophila* and other Dipteran insects lacked CSA and CSB (5, 12, 13) and UVSSA (25) orthologs. However, it was also pointed out that in the absence of TCR, RNAPII stalled at damage sites in the TS would be expected to interfere with excision repair, as has been shown in *E. coli* (26), resulting in preferential repair of the NTS (5), which was not observed (6–10). To clarify these conflicting observations and theoretical expectations, we analyzed our XR-Seq data from S2 cells to obtain a global view of strand-specific repair of the *Drosophila* genome.

From our genomic repair maps of *Drosophila*, we initially focused on the *betaTub60D* and *ade3* genes for TCR analysis because the lack of strand-specific repair in these genes, as determined by Southern blotting, was considered definitive evidence for lack of TCR in *Drosophila* (6–8). Fig. 3*A* shows screenshots of repair of the *betaTub60D* and *ade3* genes in *Drosophila* as well as the human orthologues of these genes (*TUBB3* and *GART*, respectively) in NHF1 and CSB cells, and Fig. 3*B* shows quantitative analysis of the TS and NTS repair of these genes. As is visually apparent from the screenshots, the TS of *betaTub60D* is repaired more efficiently than the NTS. A similar result is seen with repair of *ade3*. The quantitative data for TS and NTS reads in Fig. 3*B* clearly show that *Drosophila* performs TCR similar in magnitude to that seen in NHF1 human cells. A gene-by-gene survey of the genomic repair map (not shown) reveals varied levels of TCR in many but not all *Drosophila* genes, presumably reflecting varied levels or absence of transcription. For comparative purposes, Fig. 3 shows a screenshot and quantitation of repair for a *Drosophila* gene, *CG10348*, in which TCR is essentially absent.

Interestingly, in CSB cells (Fig. 3), there is not only a lack of TCR, but a preferential repair of the NTS in both the *TUBB3* and *GART* genes. This result parallels the preferred NTS repair seen in *E. coli* cells lacking the TCR factor Mfd (27). This result in CSB cells is consistent with inhibition of repair by the stalled polymerase and merits more systematic investigation.

Genome-wide TCR in Drosophila

To examine TCR in a large sample of *Drosophila* genes, we analyzed the CPD repair of all nonoverlapping genes over 1 kbp (5,706 genes). The results are shown in Fig. 4*A*, with results for different repair time points for S2 cells in the *top row*, and corresponding time points for NHF1 cells (10,100 genes over 5 kbp) in the *row below*. Each *panel* illustrates the averaged repair from the transcription start site (TSS) to the transcription end site (TES) for all of the genes considered, plus the average repair 2 kbp upstream and downstream. As is clear from this figure, in both species, TCR across the gene bodies appears to have begun by 10 min, and TS repair is dominant at 30–36 min. The magnitudes of TCR in human and *Drosophila* cell lines are at comparable levels. At later time points, after the TS is cleared of damage, the preference shifts to the NTS strand. It takes longer to clear TS damage (over 8 h) in human cells, probably due to longer genes in humans. The robust TCR signal exhibited by S2 cells, which lack CS proteins, contrasts starkly with the complete absence of TCR in mutant human CSB cells, which are compared with NHF1 cells in Fig. 4*B*. In fact, the CSB cells exhibit a trend toward preferential NTS repair, as seen in the individual *TUBB3* and *GART* genes (Fig. 3).

An interesting difference between the human and *Drosophila* repair profiles is seen in Fig. 4. As reported previously for NHF1 cells (20), and seen here at the 36-min and 1-h time points, there is a switch in strand preference for repair, from TS within the gene body to the NTS immediately upstream of the TSS. This is because of the well-known fact that upstream of the mammalian TSS, there is promoter- and enhancer-specific transcription "antisense" relative to the gene body (28). These "antisense" transcripts are not found in *Arabidopsis* (24), and our data suggest that they are absent in *Drosophila* as well. Instead, a dip in repair of both strands is observed immediately upstream of the TSS in *Drosophila*, presumably because of interference by transcription factors bound immediately upstream of coding sequences.

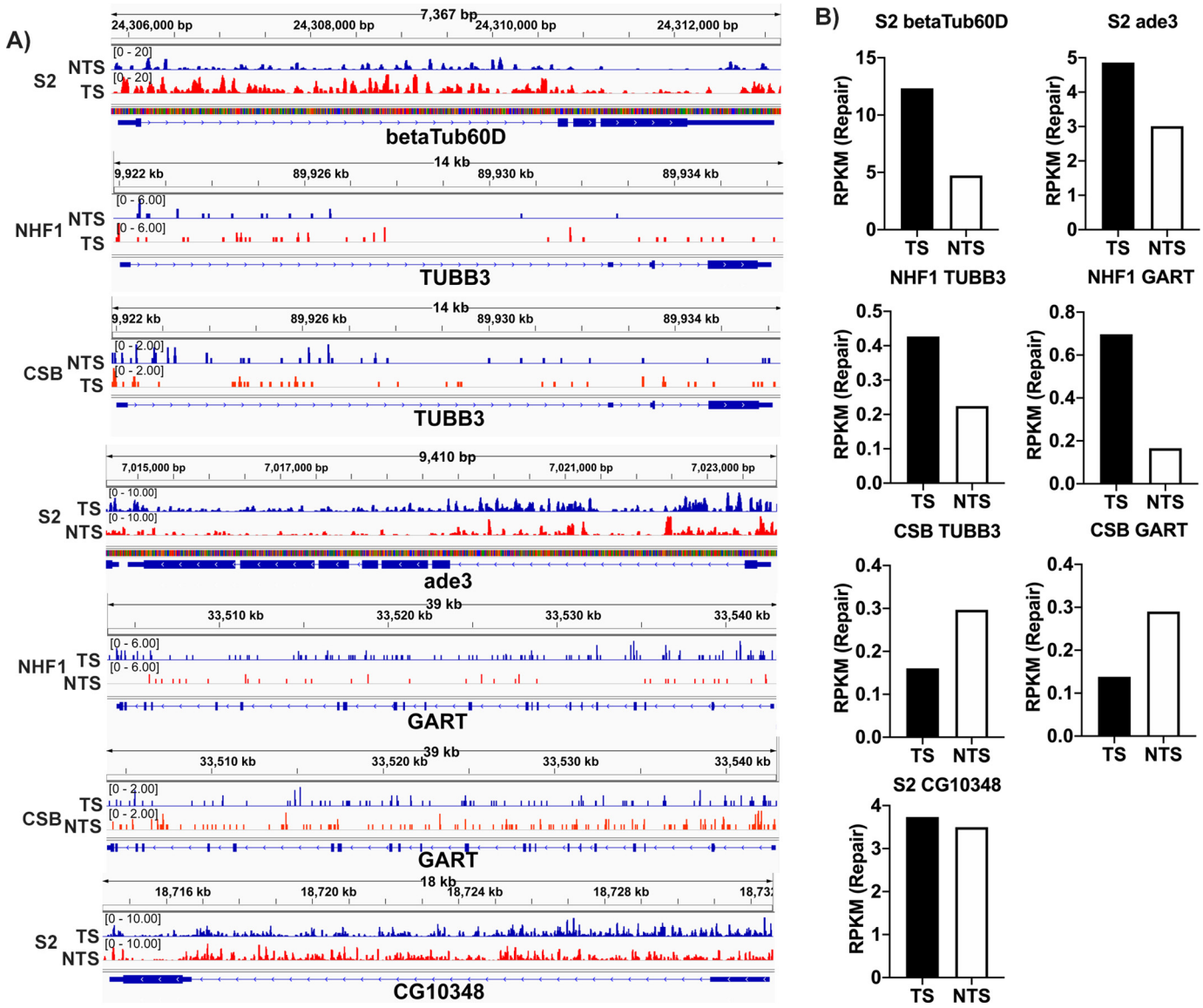

Figure 3. Transcription-coupled repair in human NHF1 and *Drosophila* S2 cells at the single gene level. Screenshots (*A*) of XR-Seq data of select genes are shown along with quantitative analysis (*B*) of the read numbers. Genes analyzed include the *betaTub60D* gene from *Drosophila* and the human ortholog *TUBB3*, as well as the *Drosophila ade3* gene and the human ortholog *GART*. Preferential repair in the TS as compared with the NTS of these genes is seen in the S2 and NHF1 cells but is absent in CSB cells, which in fact show the opposite preference, perhaps due to inhibition of TS repair by RNAP stalled at the damage. The *Drosophila CG10348* gene is also analyzed in the *bottom panels* of *A* and *B* to illustrate an example of the absence of TCR. The *y* axis in each case is RPKM. The repair signal for *Drosophila* appears stronger because it has a much smaller genome and thus more reads per kbp per million reads. Time points are 30 min (S2 cells), 36 min (NHF1), and 1 h (CSB).

Discussion

Contrary to the view held for nearly 3 decades, we show that *Drosophila* performs TCR. In fact, the magnitude of the TS/NTS repair ratio in transcribed genes is comparable to the ratios of corresponding genes in human cells. We ascribe the previous failure to observe TCR in *Drosophila* partly to the limitation of the T4 endonuclease V digestion/Southern assay used in previous studies. An important additional consideration is the particular time points at which repair was analyzed. The earliest repair time point commonly used in the previous studies was 4 h post-UV treatment (6–10). TCR may be detected in mammalian cells following 4 h of repair (Fig. 4); however, in yeast, which have much smaller genes, TCR is complete within 1 h (22). It appears that a similar rapid kinetic profile in *Drosophila*, which also has relatively small genes, likely contributes to the discrepancy between our findings and previous studies.

Our finding of TCR in *Drosophila* raises a new question: analysis of the *Drosophila* genome and the genomes of other Dipteran insects has failed to reveal CSA, CSB, or UVSSA orthologs, which are known to be essential for TCR in organisms ranging from plants to humans. The *E. coli* TCR factor Mfd, which has a different evolutionary history than CSB, exhibits considerable sequence homology in the ATPase/translocase domain of the protein. It is possible that another translocase with great sequence divergence from all known TCR translocases couples transcription to repair upon the encounter of RNAP with a transcription-blocking DNA lesion in *Drosoph-*

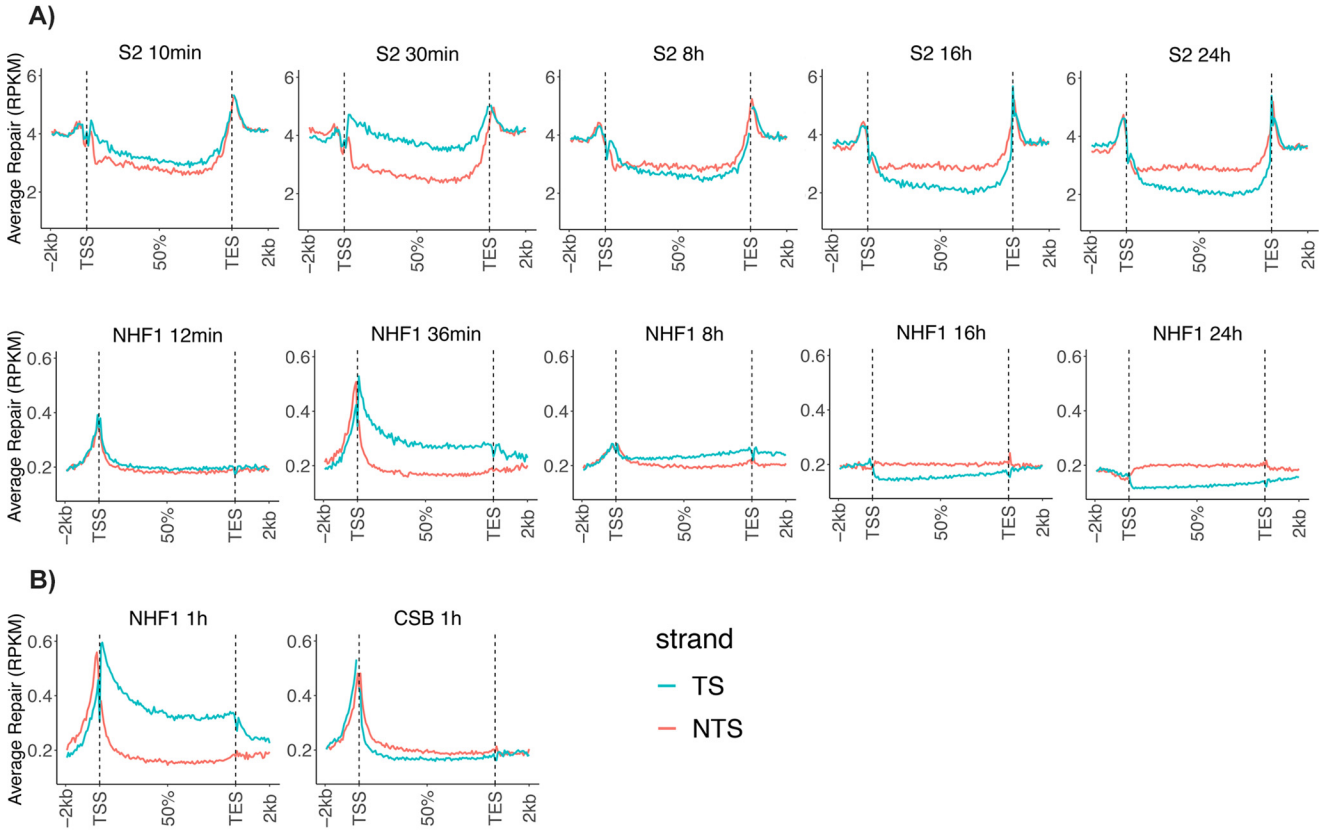

Figure 4. Genome-wide analysis of TCR of transcribed genes in *Drosophila* and human cells. *A*, comparison of *Drosophila* S2 and human NHF1 cells. XR-Seq data from the indicated time points are plotted as average repair reads RPKM (*y* axis) along the length of a "unit gene." For constructing a unit gene, a *Drosophila* data set of 5,706 genes was selected to include all genes >1 kbp with no genes that overlap or have a distance of less than 100 bp between adjacent genes. The human gene set includes 10,100 genes of >5 kbp in length with no overlaps and with a distance of at least 5 kbp between genes. For each species, the "unit gene" is 100 bins in length, and values for average repair were obtained by dividing each gene into 100 bins and averaging the repair values for each successive bin from 1 to 100. *B*, comparison of WT human NHF1 cells with cells from a patient with CSB. Data were analyzed as in *A*.

ila. In fact, in *Caenorhabditis elegans*, other chromatin-remodeling factors have been suggested to function in place of CSB for TCR during certain developmental stages (29). There is a need for further work to identify such potential transcription-coupled repair factors in *Drosophila*.

A passive mechanism for TCR has been suggested in which the stalled RNAPII reveals to the basal repair factors lesions that would otherwise be concealed by nucleosomes. This mechanism is based partly upon observations of inhibition of repair by nucleosomes, seen *in vitro* (30), and repair of transcription-blocking lesions unimpeded by the presence of the stalled RNAPII, also seen *in vitro* (11, 31–33). This particular model as related to *Drosophila* is attractive in its independence of CS proteins. Further work is needed to clarify the involvement of CS proteins in TCR as well as in the developmental deficiencies associated with Cockayne syndrome (34).

Experimental procedures

Excision and XR-Seq assays

S2-DGRC cells were obtained from the *Drosophila* Genetic Resources Center. Cells were cultured at 27 °C in Schneider's medium with heat-inactivated fetal bovine serum at 10% (v/v). For UV treatments, cells were inoculated into R-150 plates and grown to about 25–80% confluence. Medium was gently removed from the semi-adherent monolayer, cells were irradiated with UV-C, and then fresh medium containing sterilized, conditioned medium was added to cells, and cells were incubated at 27 °C. Excision assays employed 20 J m^{-2} (Fig. 1) or 10 J m^{-2} (Fig. 2), and XR-Seq assays employed 20 J m^{-2}. Following predetermined repair times, plates were placed on ice, and cooled cells were harvested by scraping and rinsing with ice-cold PBS. Cells were pelleted, transferred to Eppendorf tubes, washed with cold PBS, and resuspended in 320–340 μl of cold TE. Samples were processed for excision and XR-Seq assays as described (27), using 5 μl of RNase A and proteinase K and using 9.2% sequencing gels. For both assays, samples were immunoprecipitated with anti-CPD antibody and then either radiolabeled (excision assay) or ligated to adapters and processed for sequencing (XR-Seq). Approximately 13% of the input CPD-containing excision products are recovered using this standard excision assay/XR-Seq immunoprecipitation procedure. One plate of S2 cells per repair time point was sufficient for excision or XR-Seq assay. *Drosophila* possesses photolyases, so cells were kept in the dark or under dim yellow illumination from the time of irradiation to the time of addition of NaCl to cell lysates. XR-Seq of NHF1 (normal human fibroblast) cells was performed as described previously (4). XR-Seq analysis of CSB cell repair utilized data deposited in a prior study (20).

Data analysis

At least 6 million unique mapped reads were obtained for each sample. Analysis of sequencing reads and data visualization were as described previously (35). The alignment genome version was dm6_UCSC for S2 cells and hg38_UCSC for human cell lines. For plotting average repair profiles as a unit gene, we chose the genes with length >1 kbp for *Drosophila* and >5 kbp for *Homo sapiens*, and the distance between genes was at least 100 bp for *Drosophila* and 5 kbp for *Homo sapiens.* With these criteria, the total number of genes selected was 5,706 for *Drosophila* and 10,100 for *Homo sapiens*. Each gene was evenly divided into 100 bins from the TSS to the TES, and 2 kbp (25 bins) upstream of TSS, 2 kbp (25 bins) downstream of TES, and for each bin, from first to last, an average value for each of the selected genes was obtained and plotted. The *y* axis average reads per kbp per million total reads (RPKM) for each bin was plotted with R. The raw data and alignment data have been deposited in the Gene Expression Omnibus under accession numbers GSE76391, GSE67941, and GSE138846.

Author contributions—N. D., Y. Y., A. S., and C. P. S. conceptualization; N. D., Y. Y., A. S., and C. P. S. formal analysis; N. D., Y. Y., A. S., and C. P. S. investigation; N. D., Y. Y., and C. P. S. methodology; N. D., Y. Y., L. A. L.-B., A. S., and C. P. S. writing-original draft; N. D., Y. Y., L. A. L.-B., A. S., and C. P. S. writing-review and editing; Y. Y. data curation; Y. Y., L. A. L.-B., and C. P. S. supervision; Y. Y. and C. P. S. visualization; L. A. L.-B., A. S., and C. P. S. project administration; A. S. funding acquisition.

Acknowledgment—Cells were provided by the Drosophila Genomics Resource Center, supported by National Institutes of Health Grant 2P40OD010949.

References

1. Sancar, A. (1996) DNA excision repair. *Annu. Rev. Biochem.* **65,** 43–81 CrossRef Medline
2. Wood, R. D. (1997) Nucleotide excision repair in mammalian cells. *J. Biol. Chem.* **272,** 23465–23468 CrossRef Medline
3. Sancar, A. (2016) Mechanisms of DNA repair by photolyase and excision nuclease (Nobel Lecture). *Angew Chem. Int. Ed. Engl.* **55,** 8502–8527 CrossRef Medline
4. Hu, J., Li, W., Adebali, O., Yang, Y., Oztas, O., Selby, C. P., and Sancar, A. (2019) Genome-wide mapping of nucleotide excision repair with XR-seq. *Nat. Protoc.* **14,** 248–282 CrossRef Medline
5. Sekelsky, J. (2017) DNA Repair in *Drosophila*: mutagens, models, and missing genes. *Genetics* **205,** 471–490 CrossRef Medline
6. de Cock, J. G., Klink, E. C., Ferro, W., Lohman, P. H., and Eeken, J. C. (1991) Repair of UV-induced pyrimidine dimers in the individual genes Gart, Notch and white from *Drosophila melanogaster* cell lines. *Nucleic Acids Res.* **19,** 3289–3294 CrossRef Medline
7. de Cock, J. G., Klink, E. C., Ferro, W., Lohman, P. H., and Eeken, J. C. (1992) Neither enhanced removal of cyclobutane pyrimidine dimers nor strand-specific repair is found after transcription induction of the β 3-tubulin gene in a *Drosophila* embryonic cell line Kc. *Mutat. Res.* **293,** 11–20 CrossRef Medline
8. de Cock, J. G., Klink, E. C., Lohman, P. H., and Eeken, J. C. (1992) Absence of strand-specific repair of cyclobutane pyrimidine dimers in active genes in *Drosophila melanogaster* Kc cells. *Mutat. Res.* **274,** 85–92 CrossRef Medline
9. de Cock, J. G., van Hoffen, A., Wijnands, J., Molenaar, G., Lohman, P. H., and Eeken, J. C. (1992) Repair of UV-induced (6–4)photoproducts measured in individual genes in the *Drosophila* embryonic Kc cell line. *Nucleic Acids Res.* **20,** 4789–4793 CrossRef Medline
10. van der Helm, P. J., Klink, E. C., Lohman, P. H., and Eeken, J. C. (1997) The repair of UV-induced cyclobutane pyrimidine dimers in the individual genes Gart, Notch and white from isolated brain tissue of *Drosophila melanogaster*. *Mutat. Res.* **383,** 113–124 CrossRef Medline
11. Venema, J., van Hoffen, A., Karcagi, V., Natarajan, A. T., van Zeeland, A. A., and Mullenders, L. H. (1991) Xeroderma pigmentosum complementation group C cells remove pyrimidine dimers selectively from the transcribed strand of active genes. *Mol. Cell. Biol.* **11,** 4128–4134 CrossRef Medline
12. Sekelsky, J. J., Hollis, K. J., Eimerl, A. I., Burtis, K. C., and Hawley, R. S. (2000) Nucleotide excision repair endonuclease genes in *Drosophila melanogaster*. *Mutat. Res.* **459,** 219–228 CrossRef Medline
13. Sekelsky, J. J., Brodsky, M. H., and Burtis, K. C. (2000) DNA repair in *Drosophila*: insights from the *Drosophila* genome sequence. *J. Cell Biol.* **150,** F31–F36 CrossRef Medline
14. Hanawalt, P. C., and Spivak, G. (2008) Transcription-coupled DNA repair: two decades of progress and surprises. *Nat. Rev. Mol. Cell Biol.* **9,** 958–970 CrossRef Medline
15. Selby, C. P., and Sancar, A. (1993) Molecular mechanism of transcription-repair coupling. *Science* **260,** 53–58 CrossRef Medline
16. Selby, C. P. (2017) Mfd protein and transcription-repair coupling in *Escherichia coli*. *Photochem. Photobiol.* **93,** 280–295 CrossRef Medline
17. Xu, J., Lahiri, I., Wang, W., Wier, A., Cianfrocco, M. A., Chong, J., Hare, A. A., Dervan, P. B., DiMaio, F., Leschziner, A. E., and Wang, D. (2017) Structural basis for the initiation of eukaryotic transcription-coupled DNA repair. *Nature* **551,** 653–657 CrossRef Medline
18. Selby, C. P., and Sancar, A. (1997) Human transcription-repair coupling factor CSB/ERCC6 is a DNA-stimulated ATPase but is not a helicase and does not disrupt the ternary transcription complex of stalled RNA polymerase II. *J. Biol. Chem.* **272,** 1885–1890 CrossRef Medline
19. Epanchintsev, A., Costanzo, F., Rauschendorf, M. A., Caputo, M., Ye, T., Donnio, L. M., Proietti-de-Santis, L., Coin, F., Laugel, V., and Egly, J. M. (2017) Cockayne's syndrome A and B proteins regulate transcription arrest after genotoxic stress by promoting ATF3 degradation. *Mol. Cell* **68,** 1054–1066.e6 CrossRef Medline
20. Hu, J., Adar, S., Selby, C. P., Lieb, J. D., and Sancar, A. (2015) Genome-wide analysis of human global and transcription-coupled excision repair of UV damage at single-nucleotide resolution. *Genes Dev.* **29,** 948–960 CrossRef Medline
21. Hu, J., Choi, J. H., Gaddameedhi, S., Kemp, M. G., Reardon, J. T., and Sancar, A. (2013) Nucleotide excision repair in human cells: fate of the excised oligonucleotide carrying DNA damage *in vivo*. *J. Biol. Chem.* **288,** 20918–20926 CrossRef Medline
22. Li, W., Adebali, O., Yang, Y., Selby, C. P., and Sancar, A. (2018) Single-nucleotide resolution dynamic repair maps of UV damage in *Saccharomyces cerevisiae* genome. *Proc. Natl. Acad. Sci. U.S.A.* **115,** E3408–E3415 CrossRef Medline
23. Canturk, F., Karaman, M., Selby, C. P., Kemp, M. G., Kulaksiz-Erkmen, G., Hu, J., Li, W., Lindsey-Boltz, L. A., and Sancar, A. (2016) Nucleotide excision repair by dual incisions in plants. *Proc. Natl. Acad. Sci. U.S.A.* **113,** 4706–4710 CrossRef Medline
24. Oztas, O., Selby, C. P., Sancar, A., and Adebali, O. (2018) Genome-wide excision repair in *Arabidopsis* is coupled to transcription and reflects circadian gene expression patterns. *Nat. Commun* **9,** 1503 CrossRef Medline
25. Al Khateeb, W. M., Sher, A. A., Marcus, J. M., and Schroeder, D. F. (2019) UVSSA, UBP12, and RDO2/TFIIS contribute to *Arabidopsis* UV tolerance. *Front. Plant Sci.* **10,** 516 CrossRef Medline
26. Selby, C. P., and Sancar, A. (1990) Transcription preferentially inhibits nucleotide excision repair of the template DNA strand *in vitro*. *J. Biol. Chem.* **265,** 21330–21336 Medline
27. Adebali, O., Chiou, Y. Y., Hu, J., Sancar, A., and Selby, C. P. (2017) Genome-wide transcription-coupled repair in *Escherichia coli* is mediated by the Mfd translocase. *Proc. Natl. Acad. Sci. U.S.A.* **114,** E2116–E2125 CrossRef Medline
28. Core, L. J., Martins, A. L., Danko, C. G., Waters, C. T., Siepel, A., and Lis, J. T. (2014) Analysis of nascent RNA identifies a unified architecture of

initiation regions at mammalian promoters and enhancers. *Nat. Genet.* **46,** 1311–1320 CrossRef Medline

29. Lans, H., Marteijn, J. A., Schumacher, B., Hoeijmakers, J. H., Jansen, G., and Vermeulen, W. (2010) Involvement of global genome repair, transcription coupled repair, and chromatin remodeling in UV DNA damage response changes during development. *PLoS Genet.* **6,** e1000941 CrossRef Medline
30. Hara, R., Mo, J., and Sancar, A. (2000) DNA damage in the nucleosome core is refractory to repair by human excision nuclease. *Mol. Cell. Biol.* **20,** 9173–9181 CrossRef Medline
31. Selby, C. P., Drapkin, R., Reinberg, D., and Sancar, A. (1997) RNA polymerase II stalled at a thymine dimer: footprint and effect on excision repair. *Nucleic Acids Res.* **25,** 787–793 CrossRef Medline
32. Tremeau-Bravard, A., Riedl, T., Egly, J. M., and Dahmus, M. E. (2004) Fate of RNA polymerase II stalled at a cisplatin lesion. *J. Biol. Chem.* **279,** 7751–7759 CrossRef Medline
33. Lainé, J. P., and Egly, J. M. (2006) Initiation of DNA repair mediated by a stalled RNA polymerase IIO. *EMBO J.* **25,** 387–397 CrossRef Medline
34. Brooks, P. J. (2013) Blinded by the UV light: how the focus on transcription-coupled NER has distracted from understanding the mechanisms of Cockayne syndrome neurologic disease. *DNA Repair* **12,** 656–671 CrossRef Medline
35. Yang, Y., Adebali, O., Wu, G., Selby, C. P., Chiou, Y. Y., Rashid, N., Hu, J., Hogenesch, J. B., and Sancar, A. (2018) Cisplatin-DNA adduct repair of transcribed genes is controlled by two circadian programs in mouse tissues. *Proc. Natl. Acad. Sci. U.S.A.* **115,** E4777–E4785 CrossRef Medline

ASBMB